Mark Milman x 43627

White Light Modeling, Algorithm Development, and Validation on the Micro–Arcsecond Metrology Testbed

Mark H. Milman, Martin Regher, and TsaePyng Shen
Jet Propulsion Laboratory,
California Institute of Technology,
Pasadena, CA 91109.

Abstract

The Space Interferometry Mission (SIM), scheduled for launch in early 2010, is an optical interferometer that will perform narrow angle and global wide angle astrometry with unprecedented accuracy, providing differential position accuracies of 1uas, and 4uas global accuracies in position, proper motion and parallax. SIM astrometric measurements are synthesized from pathlength delay measurements provided by three Michelson-type, white light interferometers. Two of the interferometers are used for making precise measurements of variations in the spacecraft attitude, while the third interferometer performs the science measurement. The ultimate performance of SIM relies on a combination of precise fringe measurements of the interfered starlight with picometer class relative distance measurements made between a set of fiducials that define the interferometer baseline vectors. The focus of the present paper is on the development and analysis of algorithms for accurate white light fringe estimation, and on the preliminary validation of these algorithms on the Micro–Arcsecond Testbed (MAM).

1 The Two Image Monochromatic Interferometric Model

Consider an interferometer in which the total photon flux at the two outputs of the combiner is such that it generates a current $2I_0$ in the detector. This total photon flux is split between the two combiner outputs in a manner which depends on the total delay, so that in a time interval τ the number of photoelectrons on the two sides of the combiner is

$$N_{\pm} = N_0(1 \pm V\cos\theta) \tag{1}$$

where $\theta = \frac{2\pi D}{\lambda}$ is the phase corresponding to the total delay D, V is the visibility, λ is the wavelength, and $N_0 \equiv I_0\tau$. Now suppose we apply a triangular phase modulation, so that $\theta(t) = u(t) + \phi$, where ϕ is the (astrometric) phase being measured and $u(t)$ is the phase modulation. (For now we assume ϕ is constant during this measurement.) Then the number of electrons detected during interval i, i.e., during the i^{th} dither step of n dither steps, is

$$N_{\pm i} = \frac{N_0}{n}(1 \pm V_m\cos(u_i + \phi)) \tag{2}$$

where $u_k = (k-1)\Delta + \Delta/2 - n\Delta/2$, the effective visibility V_m is

$$V_m \equiv V\text{sinc}(\frac{\Delta}{2}), \tag{3}$$

$\text{sinc}(x) \equiv \sin x/x$, $\Delta = 2\pi s/(n\lambda)$, and s is the length of the modulation stroke. The unknown quantities in (3) are N_0, V_m, and ϕ.

Let v denote the 3–vector with components $v = (N_0,\ N_0V_m,\ \phi)$, and define the mapping $X : R^3 \to R^3$ by

$$X(v) = \frac{1}{n}(v_1, v_2\cos(v_3), v_2\sin(v_3)). \tag{4}$$

Next define the $n \times 3$ matrices A_+ and A_-,

$$A_+ = \begin{bmatrix} 1 & \cos(u_1) & -\sin(u_1) \\ \vdots & \vdots & \vdots \\ 1 & \cos(u_n) & -\sin(u_n) \end{bmatrix}, \qquad A_- = \begin{bmatrix} 1 & -\cos(u_1) & \sin(u_1) \\ \vdots & \vdots & \vdots \\ 1 & -\cos(u_n) & \sin(u_n) \end{bmatrix}. \tag{5}$$

The n–dither-step photon counts from the "bright" and "dark" fringes are, respectively,

$$N_{\pm} = A_{\pm} X(v), \tag{6}$$

corresponding to the respective intensity models in each dither step

$$N_{\pm i} = \frac{N_0}{n}\{1 \pm V_m \cos(u_i + \phi)\}. \tag{7}$$

Representative images are shown in the figure below.

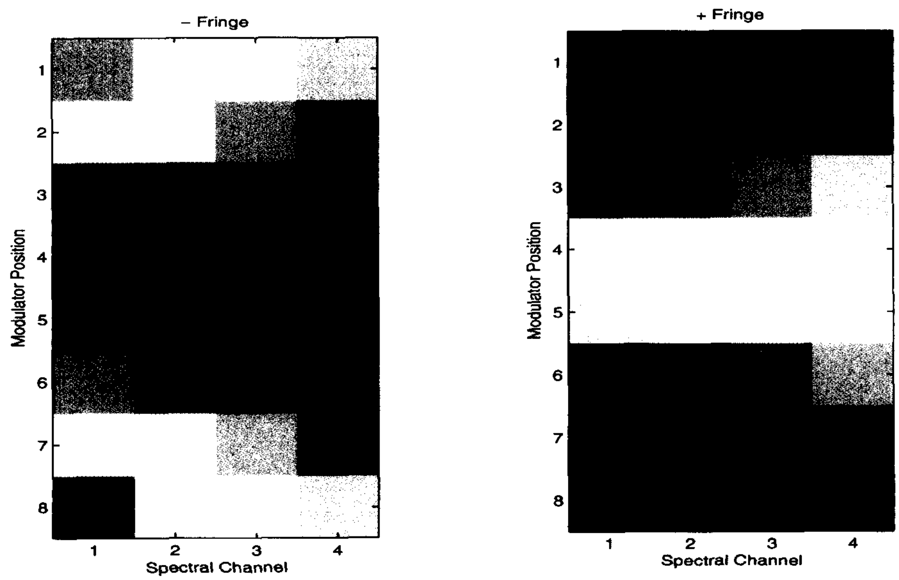

Figure 1. Two–Port Image

Define A as the concatenation of the matrices A_+ and A_-:

$$A = \begin{bmatrix} A_+ \\ A_- \end{bmatrix}, \tag{8}$$

and let N denote the concatenation of the vectors $N_{\pm}$. Then the nominal monochromatic model is

$$y = AX(v) + \eta, \tag{9}$$

where y is the observed vector of photoelectron counts and η is a zero mean random vector capturing various errors associated with detection process.

2 Phase estimators.

Since X is invertible, a broad class of estimators for the unknown parameter vector v has the general form

$$v = X^{-1}(Ky), \tag{10}$$

where K is any $3 \times n$ matrix with $KA = I$. For example the (unweighted) nonlinear least squares problem

$$\min_{v} |y - AX(v)|^2 \tag{11}$$

leads to an estimator in this class with $K = A^{\dagger}$ (the pseudoinverse of A).

The presence of the noise vector η in (10) produces an error in the estimate of v. After some analysis and algebraic manipulations the variance in the least squares delay estimate can be shown to have the final form

$$\sigma_{ls} = \frac{\lambda}{2\pi} \frac{1}{V_m \sqrt{SN_0}} \sqrt{\frac{1 + f\cos(2\phi)/n}{1 - f^2/n^2}}, \tag{12}$$

where S is the ratio of the shot noise to the total noise

$$S \equiv \frac{N_0}{N_0 + n\sigma_n^2}, \tag{13}$$

and the parameter f is defined as

$$f = \frac{\sin(2\pi\gamma)}{\sin(2\pi\gamma/n)}; \quad \gamma \equiv s/\lambda. \tag{14}$$

The ratio under the radical in (12) illuminates the delay error as a function of the number of temporal bins and the ratio between the stroke length and wavelength. For example if $\gamma = 1$, corresponding to equal wavelength and stroke length, $f = 0$ so that the ratio is one and the error is independent of the delay. In general this is not true and the error is a function of the phase offset. One simple conclusion drawn from (12) is to choose a stroke length to maximize $1 - f/n$ over the operating wavelengths of the interferometer. The figure below compares the performance of three designs with respect to this function over a 400nm–900nm bandwidth.

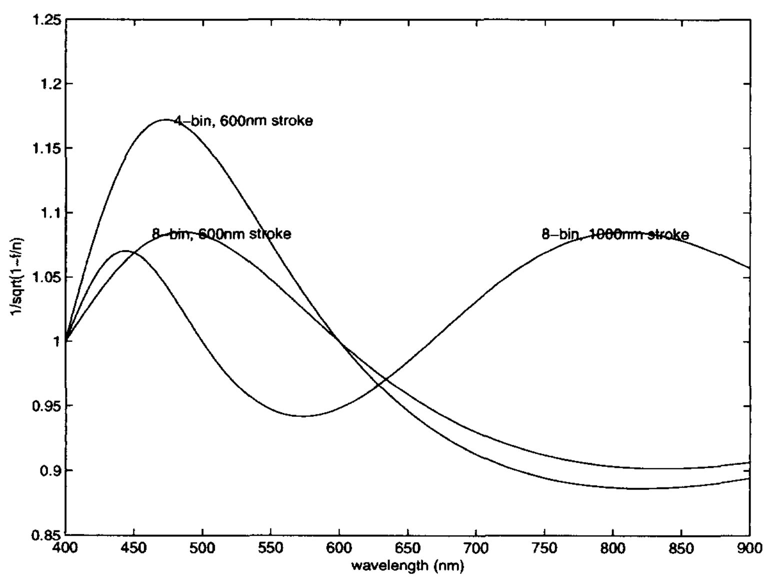

Figure 2. Comparison of performance for three estimator design parameters

A similar computation for the error variance can be made for the minimum variance estimate. This estimate is obtained from the least squares problem (11) weighted by the inverse of measurement covariance matrix. The corresponding error is

$$\sigma_{mve} = \frac{\lambda}{2\pi} \frac{1}{V_m \sqrt{2 N_0 S}} \sqrt{\left[\frac{1}{n} \sum_{i=1}^{n} \frac{\sin^2 u_i}{1 - S^2 V_m^2 \cos^2 u_i} \right]^{-1}} \tag{15}$$

Figure 3 plots the ratio $\sigma_{ls/\sigma_{mve}}$ as a function of the product VS for an 8 dither step design. Observe that as $VS \to 0$, this ratio goes to 1, while as $VS \to 1$ and $n \to \infty$, the ratio tends to $2/(1 - \mathrm{sinc}(2\pi\gamma))$. For nominal values of visibility, shot noise, and read noise for the SIM guide interferometers ($VS = .38$), there is a small (2%) advantage in using the minimum variance solution versus the least squares solution.

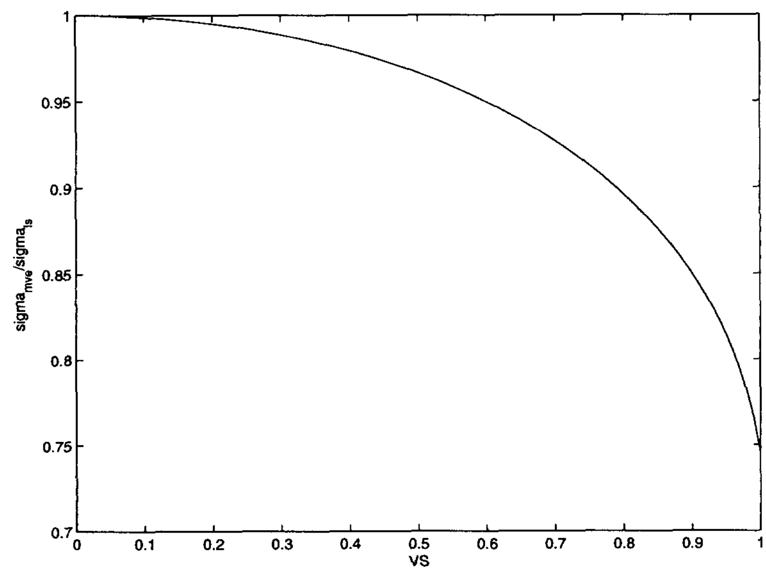

Figure 3. Ratio of $\sigma_{ls/\sigma_{mve}}$ as a function of VS

3 Improving estimates.

Several factors can degrade the performance of monochromatic estimators. For SIM applications these most notably include low SNR for the guide interferometers (because they operate at 1Khz), and vibrations or imperfections in the modulation. On MAM the most serious problem is due to vibration, which essentially produces a change in the phase while it is being estimated. Because phase estimation algorithms typically model the phase as having a constant value over the measurement period, an error results in the estimate. In the frequency domain the error in the phase estimate due to vibrations can be characterized by the following "transfer function" (shown for the least squares eight temporal bin algorithm)

$$H_T(\omega) = \sum_j a_j \mathrm{sinc}\left(\frac{\omega + \omega_j}{\frac{2}{MN\tau}} \right). \tag{16}$$

An amplitude plot of this function is shown in the figure below. Note the magnitude of the peaks, especially around twice the modulation frequency.

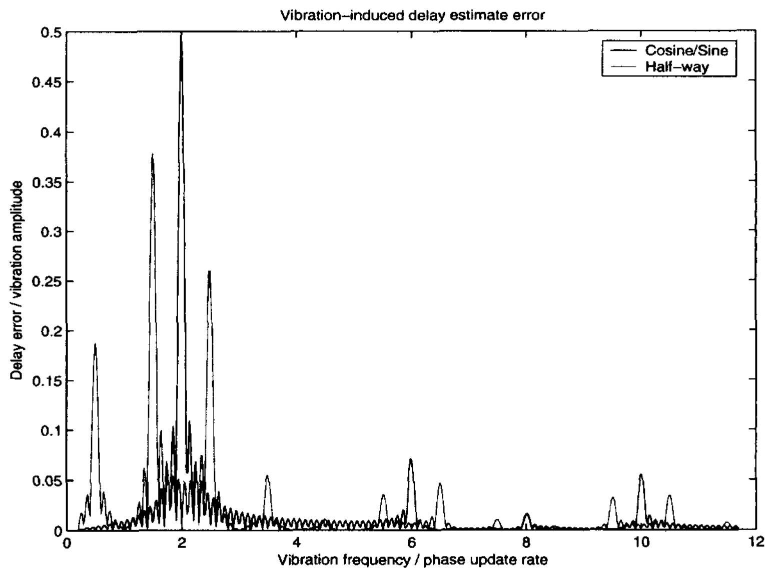

Figure 4. Phase estimation error as function of ratio of vibration frequency and phase update rate

The dominant errors of this kind for the SIM guide interferometers are changes in the internal pathlength due to vibration of the optical train and modulator non–idealities. However, these changes are monitored by the internal metrology system. A correction of the phase estimate based on metrology measurements is outlined below.

The model including the pathlength change $r(x)$ during the phase measurement is

$$N_{\pm i} = \int_{x_i-\Delta/2}^{x_i+\Delta/2} I_0\{1 \pm V\cos(kx + kr(x))\}dx, \tag{17}$$

where $\Delta = s/n$ and $r(x)$ is the change in pathlength during fringe estimation that we are trying to compensate for using metrology measurements. The quantity we wish to estimate is $\bar{r}$, the average value of r over the fringe estimation period (or the phasor quantities associated with this mean pathlength difference). To this end let $\delta(x) = r(x) - \bar{r}$ and expand the integrand above about $kx + k\bar{r}$. Retaining only terms that are linear in $\delta(x)$ leads to the model

$$N_{\pm} = A_{\pm}X(v) - B_{\pm}X(v), \tag{18}$$

where the i^{th} row of the matrix $B_{\pm}$ is

$$B_{\pm i} = \pm\begin{bmatrix} 0 & \int_{x_i-\Delta/2}^{x_i+\Delta/2}\sin(kx)k\delta(x) & \int_{x_i-\Delta/2}^{x_i+\Delta/2}\cos(kx)k\delta(x)\end{bmatrix}. \tag{19}$$

Concatenating the $\pm$ quantities as before yields

$$y = AX(v) - BX(v) + \eta. \tag{20}$$

The matrix A is constant and independent of the variation $\delta(x)$, while B is a function of the variation. Let K be any matrix such that $KA = I$, i.e. K is an unbiased estimator of $X(v)$ (assuming $B = 0$.) Let $\hat{X}(v)$

denote the nominal estimate of X without the measurement matrix B. Then the updated estimate using the measurement is obtained as (to first order approximation)

$$\hat{X}_+(v) = \hat{X}(v) + KB\hat{X}(v). \tag{21}$$

Hence the sought after perturbation is simply $KB\hat{X}(v)$.

Implementing this update depends on how B is approximated. Next we will perform this approximation with the assumption that the metrology measurements are sampled at the camera rate:

$$\delta_i = \frac{1}{\Delta}\int_{x_i-\Delta/2}^{x_i+\Delta/2} \delta(x)dx, \quad i = 1, ..., n. \tag{22}$$

Thus we can think of the n measurements made by metrology during the period of a single fringe measurement as a mapping m :

$$m(\delta(x)) = \frac{1}{\Delta}(\int_{x_1-\Delta/2}^{x_1+\Delta/2} \delta(x)dx, ..., \int_{x_n-\Delta/2}^{x_n+\Delta/2} \delta(x)dx). \tag{23}$$

Given the measurement vector there is no unique way of reconstructing the function that produced it. However, it can be shown that defining m^{-1} as the mapping that takes the measurement vector $(\delta_1, ..., \delta_n)$ to the step function $\tilde{\delta}$ that has the value δ_i on the interval $x_i - \Delta/2 \leq x \leq x_i + \Delta/2$ is optimal in a certain sense. In this case we obtain the implementation

$$B_{\pm i} = \pm [0 \quad 2\delta_i \sin(\Delta k/2)\sin(kx_i) \quad 2\delta_i \sin(\Delta k/2)\cos(kx_i)]. \tag{24}$$

This method for correcting phasors was applied to MAM testbed data. MAM experiences relatively large vibrations in a frequency regime near the sampling frequency. The figure below contains plots of the Allan Variance of the error for three cases: (i) no correction for vibration data, (ii) a full update of the A matrix using metrology (this entails recomputing the pseudoinverse with each set of metrology measurements), and (iii) the phasor correction algorithm above. As can be seen the two methods that use metrology data outperform the white light measurement scheme without correction quite significantly below 1Hz.

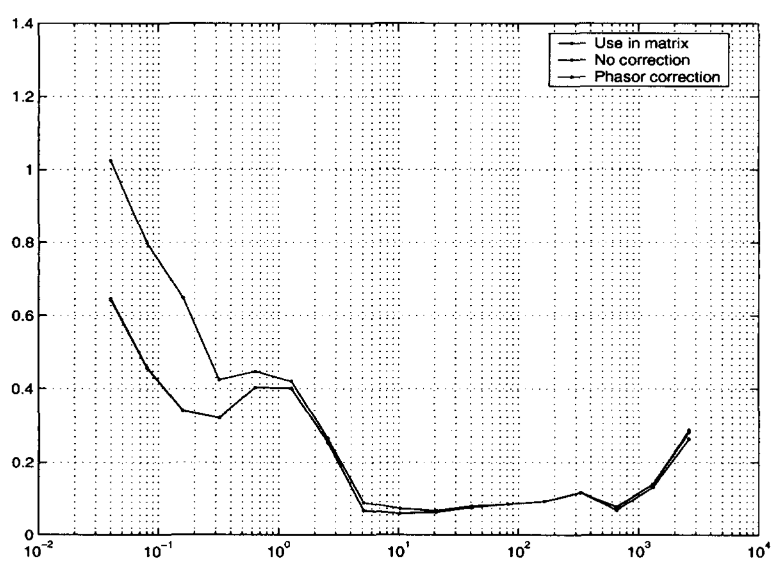

Figure 5. Vibration correction methods applied to MAM data.

An alternative to the phasor/phase correction method above, that seeks to reduce the error with each fringe measurement, is to reduce the average error over an ensemble of measurements. This latter approach is actually more aligned with the relevant astrometric metrics for SIM fringe estimation performance and may offer potential advantages as it has the capability to selectively remove the peak sensitivities in Figure 4. This work is ongoing.

4 Concluding remarks.

Precision white light interferometry is an essential technology for the success of the Space Interferometry Mission and presents many unique challenges. This paper has treated in a unified way the most pertinent aspects of quasi–monochromatic light fringe estimation in the anticipated SIM environment wherein errors due to low light levels, vibration sources, and non–ideal phase modulator behavior compromise interferometer performance. The applicability of the methods developed were demonstrated through analysis and experimental validaition on the MicroArcSecond Metrology Testbed. The next challenge in white light fringe estimation is to extend these techniques to the non–monochromatic problem.

Acknowledgment

This work was prepared at the Jet Propulsion Laboratory, California Institute of Technology, under a contract with the National Aeronautics and Space Administration.

References

[1] R. Danner and S. Unwin, eds., "Space Interferometry Mission: Taking the Measure of the Universe," JPL Pub. 400–811, Pasadena, CA, 1999.

[2] R. A. Laskin, "SIM technology development overview," in Interferometry in Space, Proc. SPIE 4852, pp. 16–32, 2003.

[3] B. E. Hines, C. E.Bell, R. Goullioud, R. Spero, G. W. Nest, T.J. Shen, E. E. Bloemhof, M. Shao, J. Catanzarite, M. Regehr, R. Machuzak, "Micro–arcsecond metrology (MAM) testbed overview," in Interferometry in Space, Proc. SPIE 4852, pp. 45–56, 2003.

[4] K. Creath, "Phase–measurement interferometry techniques," in *Progress in Optics XXVI*, Elsevier Science Pub. B. V., 1988, pp. 350–393.

[5] J. E. Greivenkamp, "Generalized data reduction for heterodyne interferometry," Optical Engineering **23**, 350-352 (1984)

[6] Mark Milman and Scott Basinger, "Error sources and algorithms for white-light fringe estimation at low light levels," Applied Optics **41**, 2655-2671 (2002)